MILLIMETER AND SUBMILLIMETER WAVE MOLECULAR BEAM MASERS

Frank C. De Lucia and Walter Gordy
Department of Physics, Duke University, Durham, NC

Molecular beam maser techniques have been developed in the shorter millimeter region and extended into the submillimeter region of the spectrum. Molecular beam oscillators with small amounts of highly stable power have been operated at 88.6 and 177.2 GHz. Amplification has also been achieved at frequencies of 57.7, 72.4, 144.8, and 317 GHz. The molecular beam maser effectively eliminates the Doppler and collision broadening which is inherent in conventional gaseous systems. The resulting high resolution has been used to achieve the most accurate measurements of molecular rotational constants to date. The rotational constant, B_0, for the ground vibrational states of $H^{12}C^{14}N$ is 44,315,975.7 ±0.4 kHz, and that of $D^{12}C^{14}N$ is 36,207,462.7 ±0.3 kHz.

I. INTRODUCTION

Several years ago in an earlier conference of this series one of us described experimental methods and spectral measurements with microwave techniques in the wavelength region of 5 to 0.5 mm [1]. A later survey of the 4 to 0.4 mm region was given at the *Fifth European Congress of Spectroscopy* [2]. These measurements were made with a crystal harmonic generator and detector with frequency markers multiplied from the standard radio frequency signals broadcast by station WWV. Our laboratory at Duke University has now extended to submillimeter-wave frequencies the operation of the valuable molecular beam maser. This maser will bring a new order of resolution and accuracy in frequency to submillimeter-wave spectral measurements, and it will provide a low-noise amplifier and an oscillator of high spectral purity (high Q) for future technological applications of submillimeter waves. So far, we have succeeded in increasing the operational frequency over previous beam masers by a factor of 3.5 in achieving maser amplification of the submillimeter-wave D_2O line at 317 GHz ($\lambda = 0.95$ mm). The results encourage us to think that we can reach still higher frequencies with this device.

As is evident from a number of other papers being presented at this conference, the optically pumped and chemically or electrically excited gaseous lasers have been successfully operated at certain submillimeter-wave frequencies. Although such devices have many potential applications and generally provide higher power than does the beam maser, they do not have the stability of frequency, the resolving power, and the low-noise figure achievable with the molecular beam maser which circumvents both Doppler and collision broadening.

The first maser to operate successfully was a molecular beam device of Gordon, Zeiger, and Townes [3], which employed the $J = 3$, $K = 3$ inversion transition of NH_3 at 24 GHz. A short-term frequency stability of 4 parts in 10^{12}, a noise figure approaching unity, and exceptionally high spectral purity were the

Presented at the Symposium on Submillimeter Waves
Polytechnic Institute of Brooklyn, March 31, April 1 and 2, 1970.

outstanding features of this new device. Since this first success in 1954, researchers have endeavored to extend the frequency range of maser operation and to expand its applications. Out of this research have come the various lasers which operate in the optical and infrared regions, the various solid state masers, and the molecular beam masers which operate in the centimeter and millimeter wave regions of the spectrum, to frequencies as high as 88.6 GHz. Table I provides a summary of molecular beam masers which have been operated in the centimeter wave region. All of the transitions on which these are based are between isolated doublet levels separated by centimeter wave frequencies. Prior to our work, only two of these molecular beam masers have been made to operate in the millimeter-wave region, both near 4 mm. Marcuse achieved beam maser operation on the 88.6 GHz transition of HCN [11-13] and Krupnov and Skvortsov, on the 72.8 GHz transition of CH_2O [14-16]. In addition to these, a number of proposals have been made to operate molecular beam masers on various types of transitions in the millimeter and submillimeter region [17-22]. To our knowledge, however, only the few listed in Table II have been successfully operated.

TABLE I. Centimeter wave molecular beam masers.

MOLECULE	FREQUENCY [MHz]	TRANSITION	REFERENCE
NH_3	24,000	various inversion transitions	a
NH_2D	18,808	$3_{13} \rightarrow 3_{03}$	b
H_2O	22,235	$6_{16} \rightarrow 5_{23}$	c
HDO	10,278	$2_{20} \rightarrow 2_{12}$	d, e
	8,578	$7_{43} \rightarrow 7_{45}$	f
D_2O	10,919	$3_{13} \rightarrow 2_{20}$	e
	10,947	$4_{14} \rightarrow 5_{32}$	f
$HD^{17}O$	10,374	$2_{20} \rightarrow 2_{12}$	g
CH_2O	14,487	$2_{11} \rightarrow 2_{12}$	d
	28,975	$3_{12} \rightarrow 3_{13}$	h
CHDO	16,038	$2_{11} \rightarrow 2_{12}$	d
HDS	11,283	$2_{20} \rightarrow 2_{21}$	d
HDSe	9,139	$2_{20} \rightarrow 2_{21}$	c

a. Gordon, Zeiger, and Townes [3].
b. Thaddeus, Krisher, and Cahill [4].
c. Bluyssen, Dymanus, and Verhoeven [5].
d. Thaddeus, Krisher, and Loubser [6].
e. Bluyssen, Verhoeven, and Dymanus [7].
f. Verhoeven, Bluyssen, and Dymanus [8].
g. Verhoeven, Dymanus, and Bluyssen [9].
h. Takuma, Shimizu, and Shimoda [10].

II. GENERAL PROPERTIES OF THE MILLIMETER AND SUBMILLIMETER MOLECULAR BEAM MASER

Since the molecular beam passes through the cavity at right angles to the direction of propagation of the microwave field, Doppler broadening is virtually

TABLE II. Operational millimeter and submillimeter molecular beam masers.

MOLECULE	FREQUENCY [MHz]	TRANSITION	REFERENCE
ND_2H	57,675	$1_{11} \longrightarrow 1_{01}$	a
DCN	72,415	$J = 1 \longrightarrow 0$	b
CH_2O	72,838	$1_{01} \longrightarrow 0_{00}$	c
HCN	88,632	$J = 1 \longrightarrow 0$	d
HCN	88,632	$J = 1 \longrightarrow 0$	b
DCN	144,830	$J = 2 \longrightarrow 1$	b
HCN	177,263	$J = 2 \longrightarrow 1$	b
D_2O	316,800	$1_{10} \longrightarrow 1_{01}$	b

a. De Lucia, Cederberg and Gordy [23].
b. De Lucia and Gordy [24].
c. Krupnov and Skvortsov [14–16].
d. Marcuse [11–13].

eliminated in the beam maser. Because the Doppler broadening increases directly with spectral frequency, this feature is of great significance for the high frequencies of millimeter and submillimeter wave spectra. Collision broadening of the lines is also negligible in the beam maser because the pressure in the molecular beam must be such that the mean free path for a molecule emerging from the beam source is greater than the distance through the cavity. As a result, the predominant line-broadening mechanism is the time of flight in the cavity. This linewidth is given to a good approximation by

$$\Delta\nu = 1/t = \bar{v}/L \quad , \tag{1}$$

where: t is the time of flight in the cavity, $\bar{v}$ is the average velocity of the molecules, and L is the distance through the cavity. For typical cases this is a $\Delta\nu$ of about 5 kHz.

Population inversion for molecular beam masers is obtained by the selective deflection of molecules according to their energy state. This is most often accomplished by the action of an inhomogeneous electric field on the dipole moment of the molecules. The electric field is usually produced by a quadrupole focuser in which the field rises from zero at the center, in approximately a linear fashion, to a maximum at the outer edges. A good approximation to this field is

$$E = E_{\max} \frac{r}{r_0} \quad , \tag{2}$$

where r_0 is the radius of the focuser. Since

$$F_r = -\frac{\partial W}{\partial r} \quad , \tag{3}$$

and since a second-order Stark effect is assumed

$$W = CE^2 \quad , \tag{4}$$

it follows that

$$F_r = \frac{-2CE_{\max}^2 r}{r_0^2} \quad . \tag{5}$$

Equation (5) indicates that for molecules in states which increase in energy with increasing electric field (C positive), the force is toward the center. Molecules in states for which energy decreases with increasing electric field (C negative) are deflected toward the outside of the state selector.

The molecular force constant, C, has been defined by Equation (4). Accurate values for it may be obtained from the theory of the molecular Stark effect; for linear and diatomic molecules in the $J = 0$ state

$$W = \frac{-\mu^2 E^2}{6hB} , \tag{6}$$

and for $J \neq 0$

$$W = \frac{\mu^2 E^2}{2hBJ(J+1)} \frac{J(J+1) - 3M_J^2}{(2J-1)(2J+3)} . \tag{7}$$

For asymmetric molecules in which $\mu E \ll W^0_{J\tau} - W^0_{J'\tau'}$,

$$W = \sum_{x=a,b,c} \frac{\mu_x^2 E^2}{2J+1} \sum_{\tau'} \frac{J^2 - M_J^2}{J(2J-1)} \frac{{}^xS_{J\tau,(J-1)\tau'}}{W^0_{J\tau} - W^0_{(J-1)\tau'}}$$

$$+ \frac{M_J^2}{J(J+1)} \frac{{}^xS_{J\tau,J\tau'}}{W^0_{J\tau} - W^0_{J\tau'}} + \frac{(J+1)^2 - M_J^2}{(J+1)(2J+3)} \frac{{}^xS_{J\tau,(J+1)\tau'}}{W^0_{J\tau} - W^0_{(J+1)\tau'}} , \tag{8}$$

where: a, b, and c are the principal axes, $W^0_{J\tau}$ is the unperturbed energy of the rotational state, and the $\Sigma_{\tau'}$ is taken over all states except $J\tau$.

For any molecule having a relatively closely spaced pair of levels which are connected by an allowed transition and are simultaneously widely spaced from all other levels connected by allowed transitions, the Stark effect is

$$W = \frac{W_1^0 + W_2^0}{2} \pm \left[\left(\frac{W_1^0 - W_2^0}{2} \right)^2 + E^2 |\mu_{12}|^2 \right]^{1/2} , \tag{9}$$

where: W_1^0 and W_2^0 are the zero-field energies and μ_{12} is the dipole transition matrix element. In this case the energy is not strictly proportional to the square of the electric field. Nevertheless, "C" can still be defined by assuming an "average" field of 50,000 V/cm. This yields

$$C = \pm \frac{|\mu_{12}|^2}{\left[\left(\frac{W_1^0 - W_2^0}{2} \right)^2 + (50{,}000)^2 |\mu_{12}|^2 \right]^{1/2}} . \tag{10}$$

This last type of Stark effect is, in fact, that most often used in molecular beam masers. Virtually all centimeter masers are based on transitions of this type. The most important factors for state selection are the amount of deflection that a molecule undergoes and whether this amount of deflection is sufficient to focus molecules in the upper state into the beam, or to remove molecules in the lower state from the beam.

A cavity of high quality is of paramount importance to the successful operation of a molecular beam maser. High Q and good transmission are two somewhat

mutually exclusive properties, both of which are important to the millimeter and submillimeter wave maser. Centimeter wave masers have used low-order-mode cylindrical cavities almost exclusively. One approach to the high-frequency maser is a simple scaling down of these cavities. Unfortunately for this approach, the Q is proportional to $\nu^{-1/2}$ the linewidth to ν, and the amount of beam admitted to the cavity to ν^{-2}. All of these factors have negative effects on the operation of a maser and contribute to the need for change to another type of cavity. The Fabry-Perot cavity has high Q, a large frontal area to admit the beam, and a sufficient spread of the microwave field along the direction of the beam to give sharp spectral lines. The large volume of the Fabry-Perot cavity cancels some of this advantage by reducing the filling factor and thus making oscillation more difficult. This disadvantage can be partially overcome by the use of a multiple beam arrangement, but usable state selector geometries continue to cause a filling factor somewhat smaller than that of the usual centimeter wave cavity. When all factors are considered, the Fabry-Perot cavity at short millimeter and submillimeter wavelengths is comparable in over-all performance to the cylindrical cavity at centimeter wavelengths and is much superior to the cylindrical cavity scaled down to the shorter wavelengths.

The Q of an unloaded Fabry-Perot cavity is easily shown to be

$$Q = \frac{\pi q}{(8\rho\varepsilon_0\omega)^{1/2}} , \tag{11}$$

where q is the number of half wavelengths between the mirrors, ω is the angular frequency of the radiation, ρ is the resistivity of the cavity mirrors, and ε_0 is the permittivity. Since, for a given separation of cavity mirrors, q is proportional to ω

$$Q \propto \omega^{1/2} . \tag{12}$$

For a cavity with flat mirrors, the resonance condition is simply

$$\frac{2d}{\lambda} = q . \tag{13}$$

When one of the mirrors has a spherical surface, the relation becomes [25]

$$\frac{4d}{\lambda} = 2q + (1 + m + n)\left[1 - \frac{4}{\pi}\tan^{-1}\left(\frac{b - 2d}{b + 2d}\right)\right] , \tag{14}$$

where $q = 2, 4, 6, \cdots$, d is the mirror spacing, b is the radius of curvature of the spherical mirror, and m and n are integers representing the number of field minima over the surface of the reflecting mirrors. The use of a long ($b \gg d$) focal length mirror results in a "harmonic series" of cavity modes very similar to those of a diatomic molecule. The resonance condition for a TE_{00q} mode reduces to

$$\frac{4d}{\lambda} = 2q + \left[1 - \frac{4}{\pi}\tan^{-1}\left(\frac{b - 2d}{b + 2d}\right)\right] . \tag{15}$$

The last term on the right reduces to a value $\ll 2q$ when $b \gg d$ and thus plays the role of the "stretching constant" for the cavity series. As a matter of practical microwave technique, this result is as important to the tuning of a

high-frequency cavity system as the harmonic series of a linear molecule is to the tuning of a waveguide absorption spectrometer. This method has the added advantage of being tunable; the "harmonic series" can be used at any frequency and is not restricted to frequencies determined by the B_0 values of available tuning molecules.

III. MOLECULAR BEAM MASER FOR MILLIMETER AND SUBMILLIMETER WAVES

A diagram of the molecular beam maser for the millimeter and submillimeter region of the spectrum is shown in Figure 1. Its operation requires a vacuum

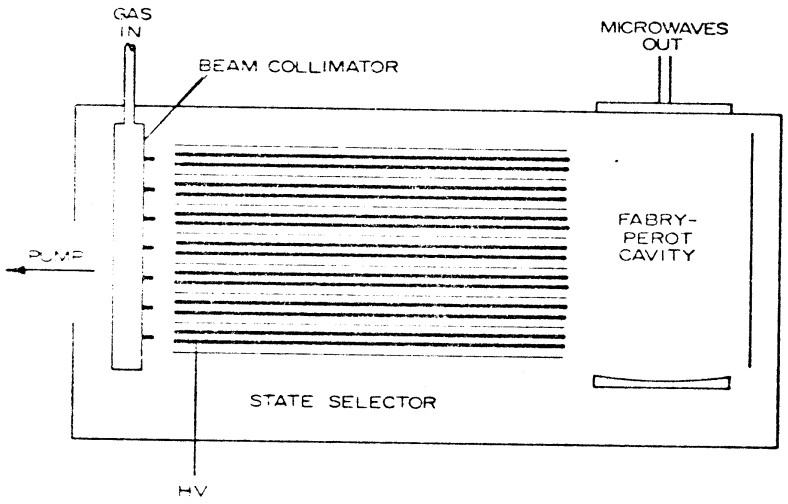

Fig. 1. Diagram of the millimeter and submillimeter molecular beam maser.

such that the mean free path of the collimated molecules with respect to the residual gases is measurably greater than the distance from the beam source to the cavity. Under this condition, the intensity of the beam will be limited only by collisions between the molecules in the beam. In round numbers, a pressure of $1 \cdot 10^{-5}$ Torr yields a mean free path of greater than 30 cm. The vacuum chamber used for these maser experiments is a rectangular box, open on top, 1 ft wide, 2 ft long, and 1 ft high. The top is formed by a piece of plexiglas 1½ in. thick. The vacuum seal is provided by a gasket held in place by a retaining lip around the inner edges of the chamber walls. Ultimately, pressures of 2×10^{-6} Torr without cold traps and $5 \cdot 10^{-7}$ Torr with liquid nitrogen trapping could be achieved.

The pumping for this vacuum chamber is provided by a CEC type PMC-720 4-in. diffusion pump with a nominal pumping speed of 500 ℓ/sec. This diffusion pump is backed by a Welch 1397 B 15 cu. ft/min fore pump. This relatively simple vacuum system and pumping equipment gives good results with a minimum of attention. During maser operation the number of molecules in the beam is far too large for any reasonable pumping system to maintain the necessary vacuum, but

cryogenic pumping provides a simple solution to this problem. Several traps, in addition to parts of the state selector, are cooled to liquid nitrogen temperature. Since most gases used in molecular beam masers have vapor pressures considerably below 10^{-6} Torr at liquid nitrogen temperature, effective pumping speeds are achieved which are greater by several orders of magnitude than those obtained by conventional pumps.

Because it is desirable to be able to state-select a wide range of transitions, a state selector providing good deflection qualities as well as a large filling factor is needed. The design used is conventional in that it employs quadrupole deflection fields. The state selector consists of seven bays of 20 rods each, biased alternately. Cooled fins extend upward between each of the bays to trap deflected and scattered molecules.

The cavity consists of two plates: one fixed, flat plate, 4 in. in diameter, with waveguide coupling, and one spherical, curved plate, 5 in. in diameter and having a focal length of 140 cm, both fabricated from copper. The spherical mirror was mounted on a slide arrangement driven by a screw which is passed through a rotary vacuum feed-through. Several flat mirrors, differing according to the size of the waveguide, were used; when high Q was required, thin irises were used to reduce the coupling.

The output power of a molecular beam maser is small, usually less than a microwatt. Therefore considerable care must be exercised in the choice, construction, and operation of the microwave detecting system. A superheterodyne system is the most sensitive detector when local oscillators of sufficient power and mixers of acceptable noise figure are available. In centimeter wave masers, superheterodyne receivers with klystrons as local oscillators and cartridge crystals as mixers have been used. The situation is similar in the long wavelength millimeter region. In the shorter millimeter region the instability and cost of fundamental frequency klystrons make harmonic generation and harmonic mixing more attractive.

When the beam maser is used for spectroscopy, both a local oscillator for the harmonic mixer and a stimulating signal for the maser cavity are required. These two signals must be separated in frequency by the i.f. so that the signal resulting from the beating in the mixer falls in the i.f. passband. Although two klystrons can be electronically locked to differ by the i.f. (or in the case of harmonic generation, the i.f. divided by the harmonic), this solution is both complicated and expensive. It has been found that for frequencies up to about 200 GHz a simple, sensitive, and stable system can be constructed which uses only one klystron. This system is shown in Figure 2. The output of the klystron is split into two parts, one of which is applied to a harmonic generator along with a 30 MHz radio frequency signal. This results in a number of output frequencies corresponding to the harmonics of the microwave signal, with sidebands at multiples of 30 MHz. Upon proper adjustment of the amplitude of the 30 MHz signal, the dc bias, and the various microwave components, adequate power can be obtained in the proper sideband. The remainder of the microwave power not applied to the harmonic generator is applied to the harmonic mixer after a small amount of this power has been coupled out by a Bethe-hole coupler. This power is used to monitor the klystron mode and to mix with the output of a frequency standard so that frequency markers and a reference signal for the klystron stabilization are provided. The

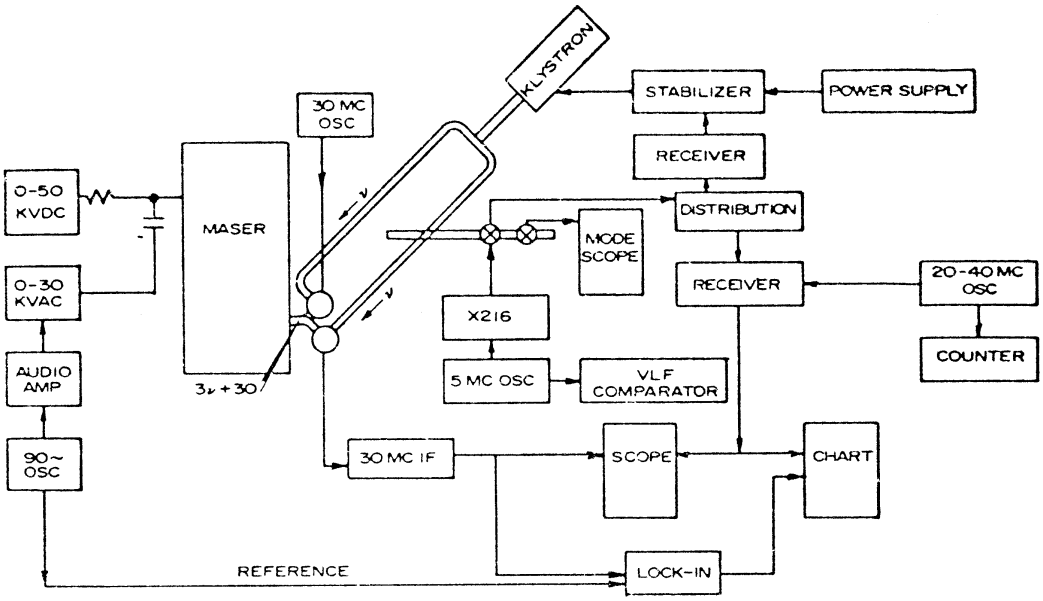

Fig. 2. Diagram of the millimeter-wave system for detection and measurement of maser output.

harmonic mixer beats the klystron signal with the maser output and converts it to the 30 MHz i.f. This signal is then amplified and detected in an i.f. strip.

IV. EXPERIMENTAL RESULTS

HCN

The maser described in the previous sections has been successfully operated on six transitions in the millimeter and submillimeter region of the spectrum. It was first operated on the hyperfine components of the $J = 1 \longrightarrow 0$ transition of HCN at 88,632 MHz. The maser was next operated on the hyperfine components of the $J = 2 \longrightarrow 1$ transition of HCN at 177,263 MHz. The hyperfine structure of

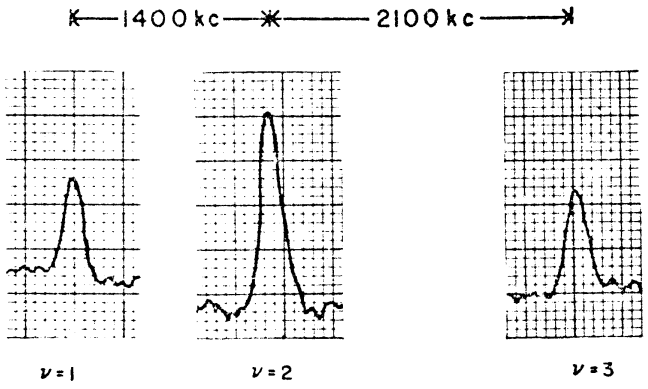

Fig. 3. Maser emission spectrum of the $J = 1 \longrightarrow 0$ transition of HCN at 88,632 MHz.

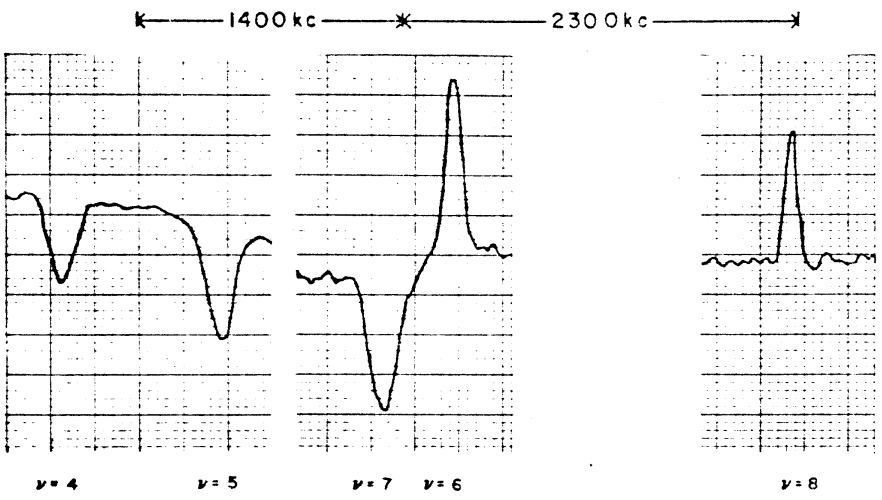

Fig. 4. Maser emission and absorption spectrum of the $J = 2 \longrightarrow 1$ transition of HCN at 177,263 MHz.

these transitions is shown in Figs. 3 and 4, respectively. Table III shows the resulting frequency measurements and spectral constants for this molecule.

In a previous section the force constants for the low J levels of HCN have been shown to be relatively large, but the Stark effect has not been considered in detail. The state selection for low J states of linear molecules differs from that of the close-lying doublets used previously for centimeter wave masers. Figure 5 shows the Stark effect for the $J = 0, 1, 2$ levels of HCN and their relative deflections in the strong field case. Since the state selection takes place at high electric field, the appropriate quantum numbers are M_I and M_J. However, the maser operates in zero field where F and M_F are the appropriate quantum numbers. Thus, if the state selection process is to be understood, the strong-field levels must be associated with the zero-field levels into which they collapse as the electric field goes from its maximum in the state selector to zero in the cavity. In principle, this can be done by solving the intermediate-field Stark effect for

TABLE III. $H^{12}C^{14}N$ spectroscopic results.

TRANSITION		OBSERVED [kHz]	CALCULATED [kHz]	DIFFERENCE [kHz]
$J = 1 \longrightarrow 0$	$F = 1 \longrightarrow 1$	88,630,415.7	88,630,414.7	1.0
	$F = 2 \longrightarrow 1$	88,631,847.3	88,631,848.3	−0.9
	$F = 0 \longrightarrow 1$	88,633,936.0	88,633,936.1	−0.1
$J = 2 \longrightarrow 1$	$F = 2 \longrightarrow 2$	177,259,676.7	177,259,677.4	−0.7
	$F = 1 \longrightarrow 0$	177,259,923.3	177,259,923.3	0.0
	$F = 2 \longrightarrow 1$	177,261,110.4	177,261,111.0	−0.6
	$F = 3 \longrightarrow 2$	177,261,223.2	177,261,222.3	0.9
	$F = 1 \longrightarrow 1$	177,263,445.0	177,263,444.7	0.3
		B_e = 44,315,975.7	± 0.4	
		D_J = 87.24	± 0.06	
		$(eQq)_N$ = −4,709.1	± 1.3	
		C_N = 10.4	± 0.3	

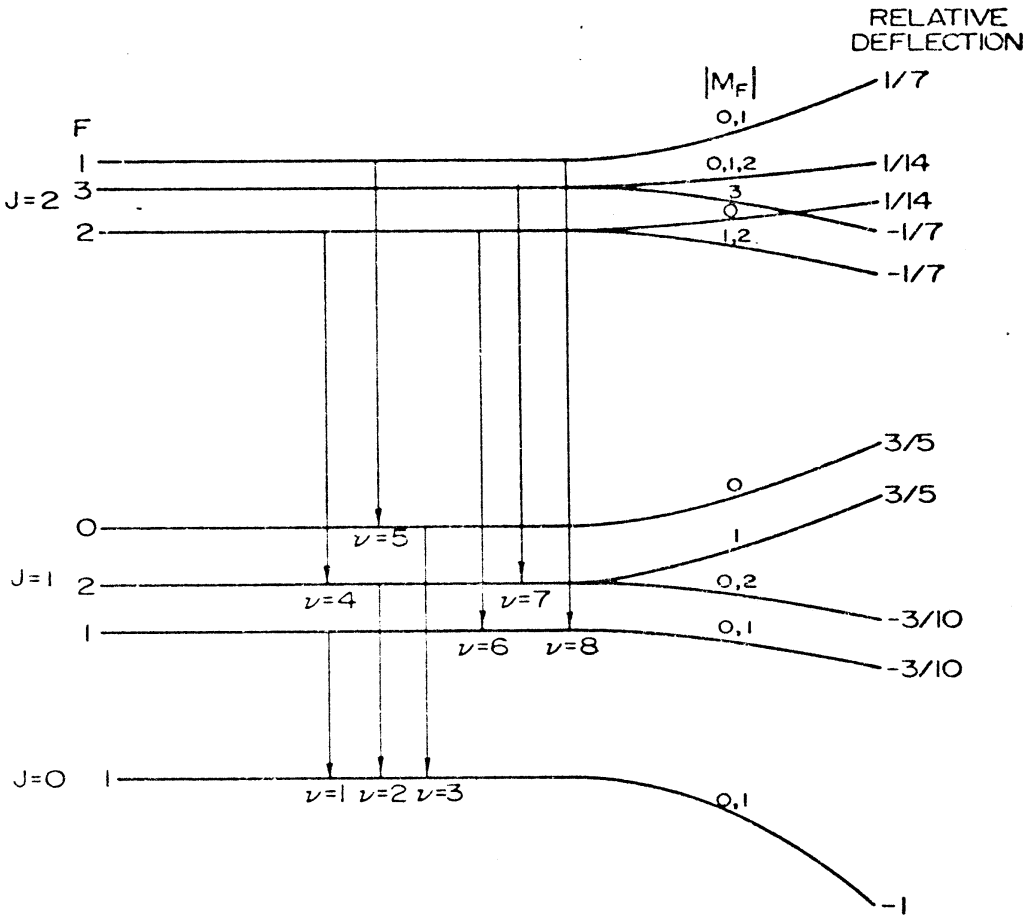

Fig. 5. Energy-level diagram showing Stark effect of HCN.

several values of Stark field and following each level from high-field to low-field approximation. There is, however, an easier method. The two following rules establish a unique correspondence between the two sets of quantum numbers: (1) $M_F = M_I + M_J = M$, (2) in the adiabatic transition from zero-field states to high-field states, those states having the same M do not cross [26].

The force constant for HCN molecules in the $J = 0$ state is approximately one and one-half times as great as that for NH_3 molecules in the $J = 3$, $K = 3$ inversion state. Thus, from Fig. 5, the transition labeled $\nu = 1$ has state selection somewhat more favorable than that of NH_3; $\nu = 2$, with parts of its upper state deflected out of the beam, about the same; and $\nu = 3$, considerably worse, because both upper and lower levels are deflected out of the beam, although the lower level, fortunately, is deflected more rapidly. The state selection for the $J = 2 \longrightarrow 1$ transition is quite interesting. All the deflections are less than those of NH_3, some considerably less. However, a new situation now occurs. Some of the $J = 2 \longrightarrow 1$ hyperfine components appear in the output as state-selected absorption lines. The transition labeled $\nu = 8$ has the ideal type of state selection for emission: the upper level is focused entirely into the beam; and the lower state, entirely out of the beam. As a result, this line is the strongest hyperfine

component in the maser output and is therefore used for the maser oscillator. This is true even though in absorption spectra it accounts for only 8% of the total transition intensity. Another emission line is $v' = 6$, with its lower level deflected entirely out of the beam and its upper level exhibiting a mixed state selection. The other three components, $v' = 4$, 5, and 7, are all absorption lines. The strengths of these beam-absorption lines are considerably enhanced by the state selection process because the resulting population difference between their upper and lower states is considerably larger than the 3% provided by the Boltzmann distribution.

Both the $J = 1 \longrightarrow 0$, $F = 2 \longrightarrow 1$ transition and the $J = 2 \longrightarrow 1$, $F = 1 \longrightarrow 1$ transition were operated as maser oscillators. A composite picture of the maser oscillator outputs is shown in Figure 6. Oscillation was achieved for the

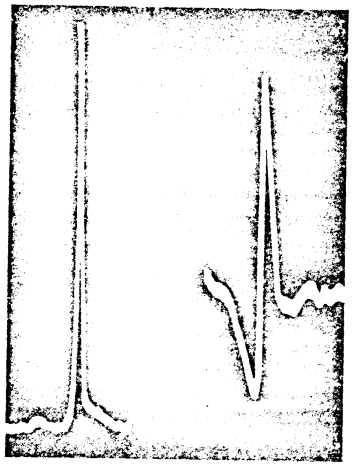

Fig. 6. Oscilloscope tracings of the output of the HCN maser oscillators at 88.6 GHz (left) and 177.2 GHz (right).

$J = 1 \longrightarrow 0$ transition with 15 kV applied to the state selector and a cavity Q of 300,000. For the $J = 2 \longrightarrow 1$ transition, 30 kV and a Q of 500,000 were used.

DCN

For determination of the spectral constants of DCN, the maser was also operated on the $J = 1 \longrightarrow 0$ and $J = 2 \longrightarrow 1$ hyperfine components of this molecule. The spectrum of the $J = 1 \longrightarrow 0$ transition of DCN is shown in Figure 7. A comparison of this spectrum with that for the $J = 1 \longrightarrow 0$ of HCN (Fig. 3) shows that the effect of the deuterium coupling is to split into triplets the levels resulting from the $F_1 = 1$ and $F_1 = 2$ states of $J = 1$. The line resulting from the $F_1 = 0$ level is not split. The experimental linewidth shown here is of the order of 10 kHz at a frequency of approximately 72,000,000 kHz. This is a better line Q than is achieved in the usual centimeter wave maser. Doppler width at this frequency is about 200 kHz, which in the usual absorption spectrometer would completely obscure the deuterium coupling and would prevent evaluation of the quadrupole coupling constant and the magnetic interaction constant. Table IV shows

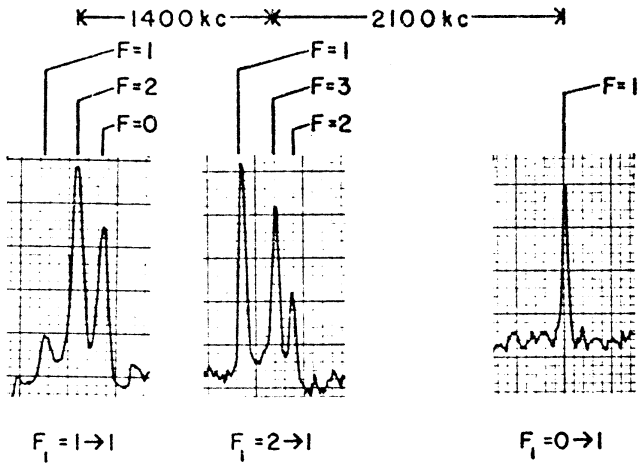

Fig. 7. Maser emission spectrum of the $J = 1 \longrightarrow 0$ transition of DCN showing the deuterium splitting of the nitrogen quadrupole lines.

TABLE IV. $D^{12}C^{14}N$ spectroscopic results.

	TRANSITION		OBSERVED [kHz]	CALCULATED [kHz]	DIFFERENCE [kHz]
$J = 1 \longrightarrow 0$	$F_N = 1 \longrightarrow 1$	$F_D = 1 \longrightarrow 0, 1, 2$	72,413,484.3	72,413,483.7	0.6
	$F_N = 1 \longrightarrow 1$	$F_D = 2 \longrightarrow 1, 2$	72,413,514.3	72,413,514.1	0.2
	$F_N = 1 \longrightarrow 1$	$F_D = 0 \longrightarrow 0, 1$	72,413,558.4	72,413,559.2	−0.8
	$F_N = 2 \longrightarrow 1$	$F_D = 1 \longrightarrow 0, 1, 2$	72,414,905.4	72,414,905.8	−0.4
	$F_N = 2 \longrightarrow 1$	$F_D = 3 \longrightarrow 2$	72,414,927.0	72,414,927.3	−0.3
	$F_N = 2 \longrightarrow 1$	$F_D = 2 \longrightarrow 1, 2$	72,414,973.2	72,414,972.4	0.8
	$F_N = 0 \longrightarrow 1$	$F_D = 1 \longrightarrow 0, 1, 2$	72,417,029.7	72,417,029.7	0
$J = 2 \longrightarrow 1$	$F_N = 1 \longrightarrow 0$	$F_D = 1 \longrightarrow 1$	144,826,841.4	144,826,841.2	0.2
	$F_N = 1 \longrightarrow 0$	$F_D = 2 \longrightarrow 1$	144,826,809.7	144,826,809.9	−0.2
		$B_0 =$	36,207,462.7 ± 0.2		
		$D_J =$	57.83 ± 0.04		
		$(eQq)_N =$	−4,703.0 ± 1.2		
		$C_N =$	8.4 ± 0.3		
		$(eQq)_D =$	194.4 ± 2.2		
		$C_D =$	−0.6 ± 0.3		

the resulting frequency measurements and spectral constants. Before our work, molecular beam masers had not been used to accurately determine the rotational constants of molecules. The values determined here for B_0 and D_J of HCN and DCN are believed to be the most accurate ever determined.

D_2O

The maser was also operated on the $1_{10} \longrightarrow 1_{01}$ transition of D_2O at 316,800 MHz. This frequency is higher than that at which the previously described superheterodyne detection system operates. For this reason, a square-law video detector was used with a corresponding decrease in sensitivity. Figure 8 shows the output of this transition.

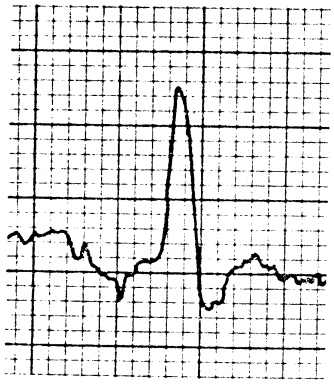

Fig. 8. Chart recorder tracing of the maser emission resulting from the $1_{10} \longrightarrow 1_{01}$ transition of D_2O at 0.95 mm wavelength.

ND_2H

The hyperfine structure of the $1_{11} \longrightarrow 1_{01}$ transition of ND_2H is considerably more complex than that of the other transitions studied. This is a direct result of the fact that all four of the nuclei of this asymmetric rotor contribute to the

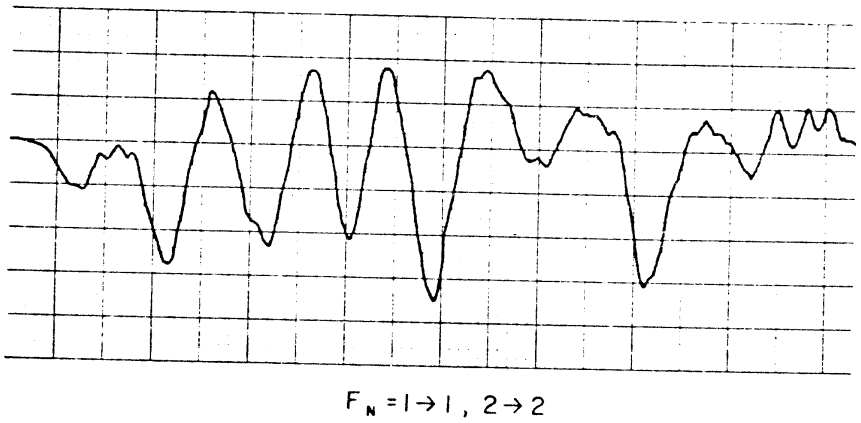

Fig. 9. Some of the maser hyperfine structure of the $1_{11} \longrightarrow 1_{10}$ transition of ND_2H.

hyperfine structure, three of them having electric quadrupole moments and all four having magnetic dipole moments. Figure 9 shows some of the resulting structure.

V. FREQUENCY AND WAVELENGTH STANDARDS IN THE MILLIMETER AND SUBMILLIMETER REGION

One of the most important requirements for the useful development of the submillimeter region of the spectrum is the existence of accurate standards of frequency and wavelength. At present, the accepted standards are transition frequencies of $^{12}C^{16}O$, $^{14}N_2{}^{16}O$, and $H^{12}C^{14}N$ [27]. These are derived from rotational spectral constants which are, in turn, derived from rotational-vibrational spectra in the near infrared. The spectral constants resulting from this beam-maser experiment are, however, considerably more precise than the infrared values; they can serve as improved standards of frequency, and when coupled with c, as wavelength standards for the far-infrared region. Table V lists a number of such transitions in which the frequencies are based on the rotational constants of $H^{12}C^{14}N$ and $D^{12}C^{14}N$.

TABLE V. Frequency and wavelength standards for the millimeter and submillimeter region as derived from the HCN and DCN rotational constants.

$J \rightarrow J+1$	FREQUENCY [GHz]	WAVELENGTH* [cm^{-1}]
	$H^{12}C^{14}N$	
0 → 1	88.6316	2.956432
1 → 2	177.2611	5.912793
2 → 3	265.8864	8.869015
3 → 4	354.5055	11.825028
4 → 5	443.1161	14.780761
5 → 6	531.7163	17.736145
6 → 7	620.3040	20.691110
7 → 8	708.8769	23.645586
8 → 9	797.4332	26.599504
9 → 10	885.9706	29.552792
10 → 11	974.4870	32.505383
	$D^{12}C^{14}N$	
0 → 1	72.4147	2.415494
1 → 2	144.8280	4.830941
2 → 3	217.2385	7.246296
3 → 4	289.6449	9.661512
4 → 5	362.0457	12.076543
5 → 6	434.4396	14.491343
6 → 7	506.8251	16.905864
7 → 8	579.2010	19.320062
8 → 9	651.5657	21.733889
9 → 10	723.9179	24.147210
10 → 11	796.2563	26.560247

*The wavelength depends on the accepted speed of light, c = 299,722.5 km/sec.

VI. OTHER POSSIBLE APPLICATIONS

Although our application of these molecular beam masers has been to achieve exceptionally high resolution spectroscopy, other applications appear promising. Theoretically, these masers should be excellent as low-noise amplifiers for technological applications where a relatively narrow bandwidth is desirable or acceptable. They may prove useful as low-noise receivers for millimeter-wave radioastronomy. They make possible a primary frequency standard for the millimeter or submillimeter wave region, one which perhaps would have greater accuracy than those now available in the lower radiofrequency region. It is probable that the frequency stability of these masers as oscillators will prove to be superior to that of the NH_3 maser. There are two major reasons for this. First, the line Q is higher because the absolute frequency is greater. More importantly, a major part of frequency instability in the NH_3 maser results from the fact that it operates on a line which is composed of unresolved hyperfine components. This is not the case for some of the maser transitions reported here which have no unresolved hyperfine structure.

ACKNOWLEDGEMENT

This work was supported by the U. S. Air Force Office of Scientific Research, Grant AF-AFOSR-66-0493B.

REFERENCES

[1] W. Gordy, *Millimeter Waves*, 1-23 (J. Fox, ed., Brooklyn, New York: Polytechnic Press, 1960).

[2] W. Gordy, *Pure and Applied Chemistry*, 11, 403-434 (London: Butterworths, 1965).

[3] J. P. Gordon, H. J. Zeiger, and C. H. Townes, *Phys. Rev.*, 99, 1264 (1955).

[4] P. Thaddeus, L. C. Krisher, and P. Cahill, *J. Chem. Phys.*, 41, 1542 (1964).

[5] H. Bluyssen, A. Dymanus, and J. Verhoeven, *Phys. Lett.*, 24A, 482 (1967).

[6] P. Thaddeus, L. C. Krisher, and J. H. N. Loubser, *J. Chem. Phys.*, 40, 257 (1964).

[7] H. Bluyssen, J. Verhoeven, and A. Dymanus, *Phys. Lett.*, 25A, 214 (1967).

[8] J. Verhoeven, H. Bluyssen, and A. Dymanus, *Phys. Lett.*, 26A, 424 (1968).

[9] J. Verhoeven, A. Dymanus, and H. Bluyssen, *J. Chem. Phys.*, 50, 3330 (1969).

[10] H. Takuma, T. Shimizu, and K. Shimoda, *J. Phys. Soc. Japan*, 14, 1595 (1959).

[11] D. Marcuse, *J. Appl. Phys.*, 32, 743 (1961).

[12] D. Marcuse, *Proc. IRE*, 49, 1706 (1961).

[13] D. Marcuse, *IRE Trans. Inst.*, 11, 187 (1962).

[14] A. F. Krupnov and V. A. Skvortsov, *Soviet Physics JETP*, 18, 74 (1964).

[15] A. F. Krupnov and V. A. Skvortsov, *Soviet Physics JETP*, 18, 1426 (1964).

[16] A. F. Krupnov and V. A. Skvortsov, *Soviet Physics JETP*, 20, 1079 (1965).

[17] F. S. Barnes, *Quantum Electronics* (C. H. Townes, ed., New York: Columbia University Press, 1960).

[18] A. I. Barchukov and A. M. Prokhorov, *Quantum Electronics* (C. H. Townes, ed., New York: Columbia University Press, 1960).

[19] R. G. Strauch, R. E. Cupp, M. Lichenstein, and J. J. Gallagher, *Quasi-Optics* (J. Fox, ed., Brooklyn, New York: Polytechnic Press, 1964).

[20] W. Gordy and M. Cowan, *J. Appl. Phys.*, **31**, 541 (L) (1960).

[21] J. B. Newman, *Advances in Quantum Electronics* (J. R. Singer, ed., New York: Columbia University Press, 1961).

[22] K. Shimoda, *Quantum Electronics* (P. Grivet and N. Bloembergen, eds., New York: Columbia University Press, 1964).

[23] F. De Lucia, J. W. Cederberg, and W. Gordy, *Bull. Am. Phys. Soc.*, **15**, 562 (1970).

[24] F. De Lucia and W. Gordy, *Phys. Rev.*, **187**, 58 (1969).

[25] G. D. Boyd and J. P. Gordon, *Bell Systems Tech. J.*, **40**, 489 (1961).

[26] V. Hughes and L. Grabner, *Phys. Rev.*, **79**, 829 (1950).

[27] K. N. Rao, C. J. Humphreys, and D. H. Rank, *Wavelength Standards in the Infrared* (New York: Academic Press Inc., 1966).